Report

Current Biology

Hippocampal Attractor Dynamics Predict Memory-Based Decision Making

Highlights

- Putative attractor dynamics were tracked using fMRI and morphed virtual environments
- Linear morphing caused nonlinear changes in hippocampal patterns and spatial memory
- The sigmoidal pattern in hippocampus scaled with the sigmoidal pattern in memory
- Remapping-like phenomenon in response to spatial context supports decision making

Authors

Ben Steemers, Alejandro Vicente-Grabovetsky, Caswell Barry, Peter Smulders, Tobias Navarro Schröder, Neil Burgess, Christian F. Doeller

Correspondence

ben.steemers@nih.gov (B.S.), christian.doeller@donders.ru.nl (C.F.D.)

In Brief

Steemers et al. combined fMRI with virtual navigation in morphed environments. Linear morphing between familiar environments caused linear changes in activity patterns in sensory cortex but commensurate nonlinear changes in hippocampal activity patterns and remembered locations, providing evidence for putative attractor dynamics in the hippocampus.

Steemers et al., 2016, Current Biology *26*, 1–8
July 11, 2016
http://dx.doi.org/10.1016/j.cub.2016.04.063

CellPress

Please cite this article in press as: Steemers et al., Hippocampal Attractor Dynamics Predict Memory-Based Decision Making, Current Biology (2016), http://dx.doi.org/10.1016/j.cub.2016.04.063

Current Biology
Report

Hippocampal Attractor Dynamics Predict Memory-Based Decision Making

Ben Steemers,[1,2,*] Alejandro Vicente-Grabovetsky,[1] Caswell Barry,[3] Peter Smulders,[1] Tobias Navarro Schröder,[1] Neil Burgess,[4,5] and Christian F. Doeller[1,*]
[1]Donders Institute for Brain, Cognition and Behaviour, Radboud University, 6525 EN Nijmegen, the Netherlands
[2]Laboratory of Neuropsychology, National Institute of Mental Health, NIH, Bethesda, MD 20892, USA
[3]Research Department of Cell and Developmental Biology, UCL, Gower Street, London WC1E 6BT, UK
[4]UCL Institute of Cognitive Neuroscience, 17 Queen Square, London WC1N 3AZ, UK
[5]UCL Institute of Neurology, Queen Square, London WC1 3BG, UK
*Correspondence: ben.steemers@nih.gov (B.S.), christian.doeller@donders.ru.nl (C.F.D.)
http://dx.doi.org/10.1016/j.cub.2016.04.063

SUMMARY

Memories are thought to be retrieved by attractor dynamics if a given input is sufficiently similar to a stored attractor state [1–5]. The hippocampus, a region crucial for spatial navigation [6–12] and episodic memory [13–18], has been associated with attractor-based computations [5, 9], receiving support from the way rodent place cells "remap" nonlinearly between spatial representations [19–22]. In humans, nonlinear response patterns have been reported in perceptual categorization tasks [23–25]; however, it remains elusive whether human memory retrieval is driven by attractor dynamics and what neural mechanisms might underpin them. To test this, we used a virtual reality [7, 11, 26–28] task where participants learned object-location associations within two distinct virtual reality environments. Participants were subsequently exposed to four novel intermediate environments, generated by linearly morphing the background landscapes of the familiar environments, while tracking fMRI activity. We show that linear changes in environmental context cause linear changes in activity patterns in sensory cortex but cause dynamic, nonlinear changes in both hippocampal activity pattern and remembered locations. Furthermore, the sigmoidal response in the hippocampus scaled with the strength of the sigmoidal pattern in spatial memory. These results indicate that mnemonic decisions in an ambiguous novel context relate to putative attractor dynamics in the hippocampus, which support the dynamic remapping of memories.

RESULTS

Participants gave written consent and were paid for participating, as approved by the local Research Ethics Committee (CMO region Arnhem-Nijmegen, the Netherlands). To create stable object-place memories, we let participants extensively learn the locations of four objects in two virtual environments (environment A and F; Figure 1) over the period of 2 days, while feedback about the correct object position was provided at the end of each trial. Performance was measured as the distance error in object replacement as a fraction of arena width. Throughout the two training sessions, participants' performance increased, reaching ceiling levels on day 2 (Figure S1A). Performance did not differ between the two environments at the end of training ($t_{19} = 1.19$, $p = 0.25$; see Figure S1).

After training, and while lying in the MRI scanner, participants were required to perform the same behavioral task in four novel "morph" environments (B through E) in addition to the known environments A and F. Crucially, the backgrounds, which distinguished the environments, varied linearly from A to F (e.g., B = 80% × A + 20% × F, C = 60% × A + 40% × F, etc.; Figure 1B). Unknown to the participants, transitions between environments were introduced during inter-trial intervals. Participants were not informed about the environmental manipulation and did not receive feedback during this session. Environments were presented in a random order (Supplemental Experimental Procedures).

To formally assess the behavioral response profile, we looked at the relative difference between the object replacement location and the true object location in environments A (ΔA) and F (ΔF), expressed as ΔA/(ΔA + ΔF). This behavioral similarity measure scales linearly from 0 to 1 with increasing ΔA and decreasing ΔF, reflecting the "A-ness" and "F-ness" of each memory response (Figure 1A). We used maximum likelihood estimates (MLE) to fit this measure to (1) a sigmoidal model indicative of putative attractor dynamics and (2) a linear control model representing the visual change in environments A to F, with model complexity held constant (both models have two free parameters; Supplemental Experimental Procedures). The similarity measure indeed followed a sigmoidal rather than a linear model (paired t test on the resulting residual sum of squares [RSS], $t_{19} = 4.62$, $p < 0.001$; Figure 1D), with the sigmoid centered between environments C and D in the majority of participants (15 out of 20; Figure 1E). On the other hand, memory confidence, measured on a five-point scale after each trial, scaled linearly with difference from either baseline environment in 87% of participants (Figure 1D). A behavioral control experiment, where naive participants judged the similarity between the background cues, showed that the sigmoidal memory response pattern was

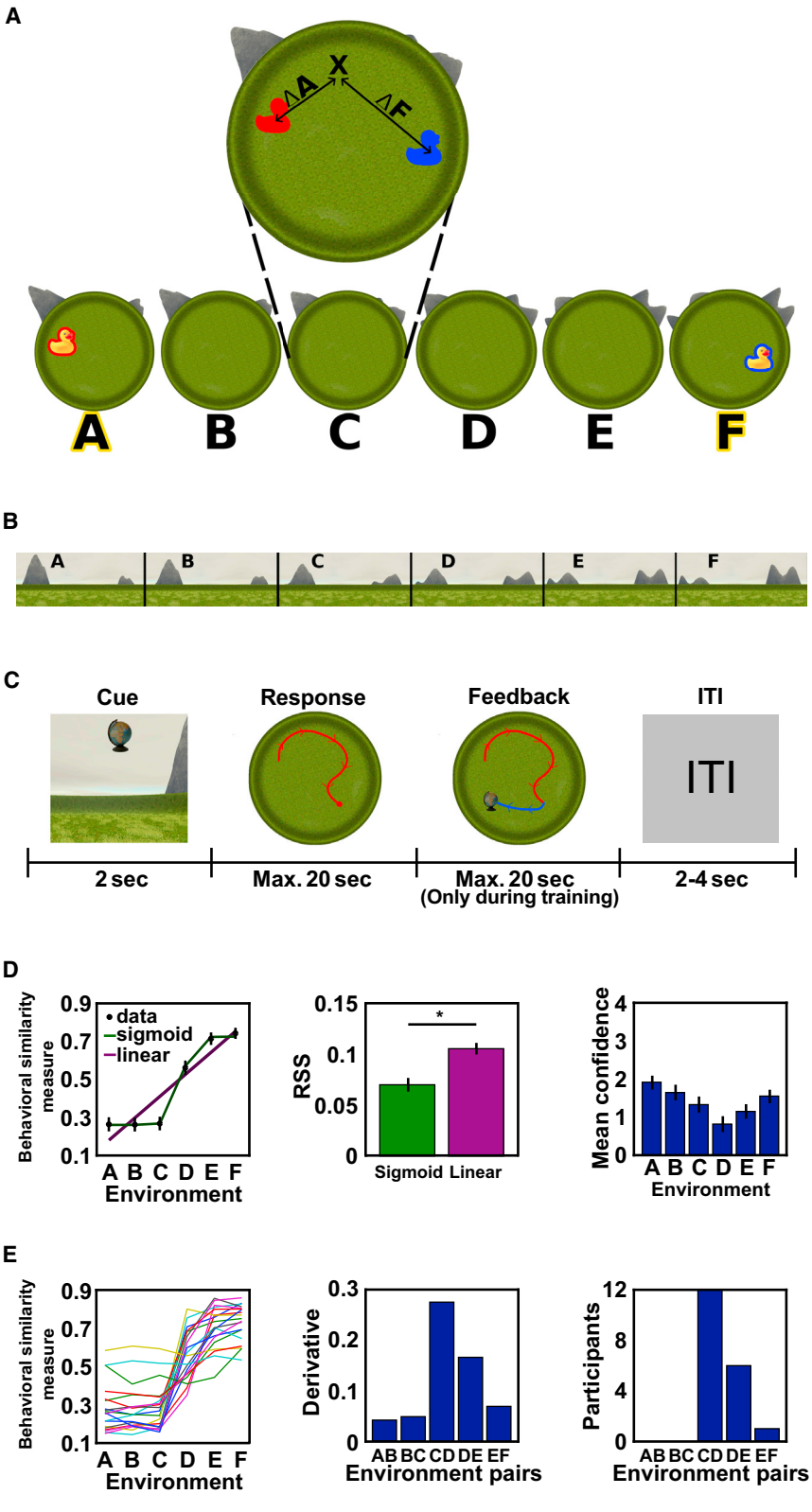

Figure 1. Memory Performance in the Virtual Reality Task

(A) Participants learned the locations of four objects in two environments (A and F); the duck depicts an example object. Subsequently, they "replaced" the objects in environments A and F and in morphed environments B, C, D, and E. For every trial, the distance of replacement locations (illustrated by "X" in the example of environment C) from the object's positions in A (ΔA, see red duck) and F (ΔF, see blue duck) was measured.

(B) Morph sequence of background cues. Morphing A into F was achieved by changing the contribution of the height maps of the mountains in the background from environment A to F in a linear fashion.

(C) In each trial, participants were cued with one of the objects, then navigated to the remembered object location, and placed the object by a button press (response). Feedback was given by showing the object in its correct location (only in the training phase).

(D) Left: the relative sizes of ΔA and ΔF (see A, expressed as ΔA/(ΔA + ΔF)) was taken as a behavioral expression of the similarity of any environment to the base environments A and F. This behavioral similarity measure is plotted separately for the different environments (averaged across trials and participants, ±SEM) along with sigmoid and linear model fit curves. Middle: bars show model fits (residual sum of squares [RSS], between model and data, ±SEM) separately for both models. The sigmoid model fits the data better than the linear model (t_{19} = 4.62, $p < 0.001$). Right: mean confidence (averaged across participants ± SEM) is plotted for each environment. ANOVA shows a significant effect of environment on confidence ($F_{(5,70)}$ = 10.92, $p < 0.001$).

(E) Left: the relative difference between the drop error in environment A (ΔA) and F (ΔF), expressed as ΔA/(ΔA+ΔF), is plotted per environment (averaged across trials), separately for each participant. Middle: mean derivatives between the responses from panel (D) between subsequent environments are plotted. The derivatives differ significantly ($F_{(4,76)}$ = 53.6, $p < 0.001$) and peak between environment C and D. Right: the highest average slope of linear fits on ΔA/(ΔA+ΔF) between neighboring environments is observed in most participants between environment C and D. For performance during the training phase, see Figure S1.

not due to differences in the perception of the backgrounds, which were judged to differ in a linear rather than a sigmoidal fashion along the morph sequence (t_{15} = 4.61, $p < 0.001$; Figure 2).

If the sigmoidal behavioral pattern reflects putative attractor dynamics in brain activity, we would expect a similar sigmoidal transition in the similarity of the multi-voxel activity patterns for the morph environments compared to the two baseline environments [29]. Since the offset of the sigmoids fitted to behavioral data differed between participants (see Figure 1E), we used each participant's behavioral response pattern to predict the similarities in multi-voxel activity patterns between pairs of environments, akin to population vector analyses of

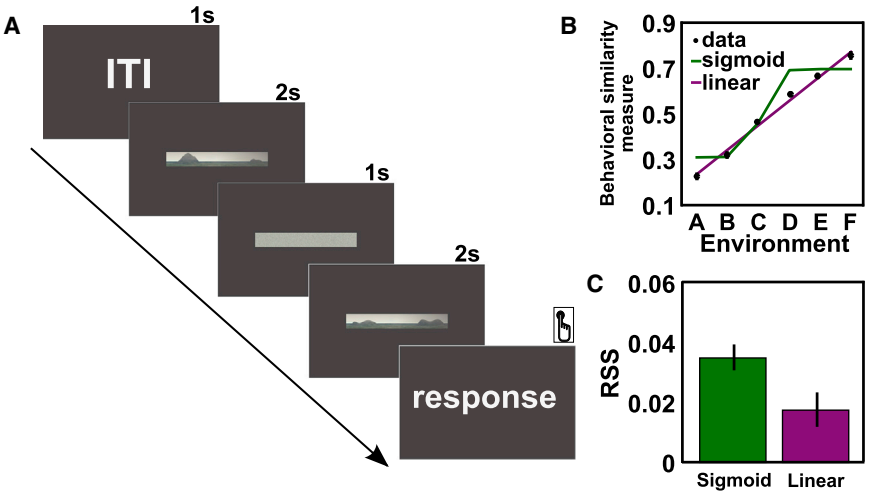

Figure 2. Perception of Environment-Specific Background Independent of Virtual Navigation

(A) Trial structure of follow-up behavioral experiment. 16 naive participants scored the similarity between pairs of background images on a five-point scale. These were the same images used to make distinguishable backgrounds in the 3D navigation task but now presented 2D.

(B) Naive similarity judgments for each environment to either environment A (ΔA) or environment F (ΔF), expressed as ΔA/(ΔA+ΔF), are plotted, along with linear and sigmoidal model fits (averaged across participants ± SEM).

(C) The measure ΔA/(ΔA+ΔF) was fitted to a linear and perfect sigmoid model using MLE, and the resulting RSS are shown (±SEM). Comparison of the residuals revealed that the linear model shows a significantly better fit than the sigmoidal model (paired t test $t_{15} = 4.61$, $p < 0.001$).

place cell firing [20] (Supplemental Experimental Procedures). We correlated the actual multi-voxel patterns for each environment-by-environment combination and tested this against the aforementioned prediction models using general linear modeling (GLM) (Figure 3A). We found a response pattern following the sigmoidal prediction obtained from each participant's behavioral response function in a hippocampal region of interest (ROI; peak coordinates x = −31, y = −26, z = −7, peak Z = 3.10 uncorrected; bootstrap corrected p = 0.036; see Figure 3B and Supplemental Experimental Procedures for details). The sigmoidal effect in the hippocampus was strongest for responses with high memory confidence (Figure 3D). No effect was found in the hippocampus for a linear model, even at a lenient uncorrected threshold of $p < 0.01$. In contrast, a linear, but not a sigmoidal, response pattern was observed in visual cortex (x = −8, y = −79, z = 11; peak Z = 3.91 uncorrected; bootstrap corrected $p < 0.01$; Figure 3C; no region outside visual cortex showed a significant linear effect at bootstrap-corrected $p < 0.05$). Additional control analyses demonstrated that the sigmoidal effect in the hippocampus was not due to differences in navigational behavior across environments (Figures S2A and S2B), differences in mean hippocampal blood-oxygen-level-dependent (BOLD) signal across environments (Figure S2C), or an effect of the similarities of behavioral response trajectories when the same object was placed across environments (Figure S3A). Finally, a consistent sigmoidal or linear response pattern was absent in the perirhinal cortex, entorhinal cortex, and parahippocampal cortex (Figure S3B), making it unlikely that our hippocampal observation is the net result of putative extrahippocampal attractor dynamics within the medial temporal lobe.

In sum, these results indicate that the neural activity pattern in the hippocampus follows nonlinear dynamics matching the behavioral response pattern. However, the presence of a sigmoidal response pattern in brain and behavioral data does not unambiguously imply that both adhere to putative attractor dynamics to a corresponding degree. To test this, we assessed the strength of the sigmoidal response profile in behavioral and fMRI data separately by fitting a "perfect," canonical, sigmoidal model using GLM to both datasets (i.e., a step function predicting immediate transition between A and F states; see Figure S4A). The resulting t values for both types of data, obtained per participant, were correlated across participants (Figure S4B). Significant correlation was seen again in the hippocampus (peak coordinates x = −29, y = −15, z = −19; peak Z = 3.79 uncorrected; bootstrap corrected p = 0.002; Figures 4A and 4B) for the perfect sigmoidal model, but the effect was absent for the linear model (even at a lenient threshold of $p < 0.01$, uncorrected). Importantly, an additional within-trial analysis showed that the ratio between linear and sigmoidal fit systematically changed between the early and the late phases of trials, reflecting a dynamic shift to a dominantly sigmoidal fit toward late trial phases (linear regression: slope = 0.004, $p < 0.005$; Figure 4C). Furthermore, Monte-Carlo simulations showed that the linear model outperforms the sigmoidal model on randomly shuffled data (Kolmogorov-Smirnov test: $p < 0.001$; Figure 4D; Supplemental Experimental Procedures). Finally, additional post hoc analyses further suggest that the behavioral and fMRI responses are both clustered around environment A or F representations (Figure 4F), indicative of a concurrent sigmoidal pattern in behavior and neural data.

DISCUSSION

Our data show that memory retrieval in ambiguous novel situations is associated with nonlinear dynamics in the hippocampus, the brain's key region for episodic and spatial memory [7, 9, 13–18, 28–30], corroborating predictions of attractor-based computational models of memory [1–4]. Our findings also dovetail with recording work in the hippocampus [20, 22] by demonstrating a nonlinear response pattern in the hippocampus as a function of linearly changing input. Furthermore, the sigmoidal response pattern in the hippocampus (1) was predominant in trials in which participants had high confidence in their memory response and (2) scaled with the strength of the sigmoidal pattern in behavior across participants. Thus, the current findings shed new light on the behavioral relevance of these hippocampal computations. That is, we demonstrate that the divergence of orthogonal, competing representations in the hippocampus directly translates into mnemonic decisions, indicative of putative attractor dynamics [13, 17, 18, 31–35].

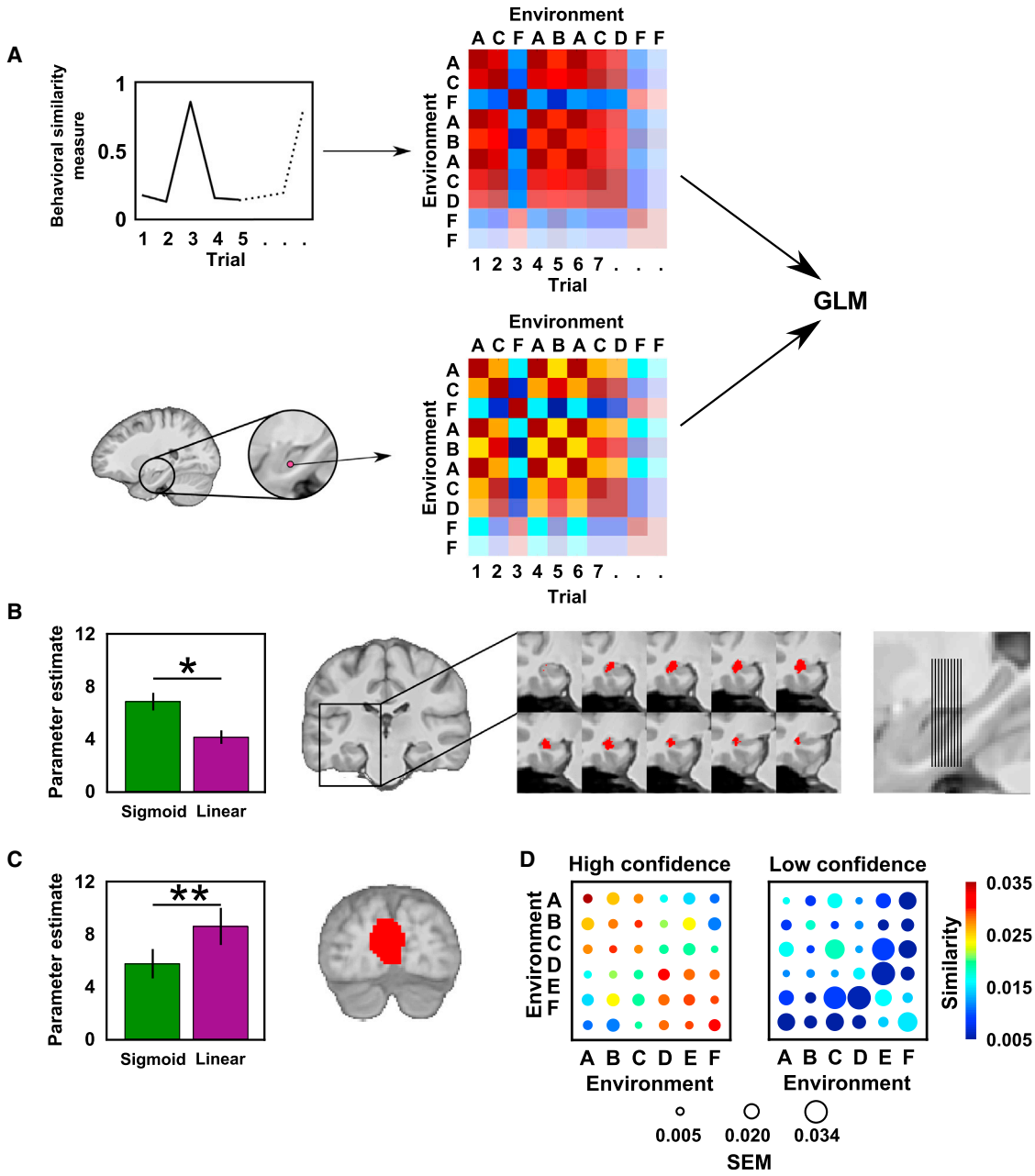

Figure 3. Sigmoidal Response Pattern in the Hippocampus

(A) Schematic of analysis logic: behavioral similarity to baseline environments (see example in top left panel) was used to generate predictor matrices for all environment pairs (top right). Multi-voxel patterns in a searchlight analysis (bottom left; see Supplemental Experimental Procedures) were correlated between trials creating a data matrix (bottom right), which was tested against the predictor matrix using GLM (see Figure S4A).

(B) Results from the behaviorally informed sigmoidal and the linear prediction model restricted to hippocampal region of interest; bars show the average effect size in the hippocampus peak ± SEM ($x = -31$, $y = -26$, $z = -7$; bootstrap corrected $p < 0.05$; see also Figure S3). Results, thresholded at a bootstrap-corrected $p < 0.05$, are overlaid on a study-specific structural template and resampled to MNI space. Depicted is the extent of the hippocampal effect from $y = -34$ to $y = -24$ with slice locations shown on a sagittal plane (right). These results were not influenced by differences in navigational behavior or mean hippocampal BOLD signal across environments (see Figure S2).

(C) Searchlight results using a linear prediction model are overlaid on an averaged structural image ($y = -85$), thresholded at bootstrap-corrected $p < 0.05$. Bars show the effect size in the peak visual cortex voxel ± SEM ($x = -8$, $y = -79$, $z = 11$; bootstrap-corrected $p < 0.005$), separately for the sigmoidal and linear model.

(D) Strength of neural similarity of hippocampal multi-voxel pattern for any environment compared to all other environments (radius of 5 mm around the peak from the sigmoid model, see B; averaged across participants). Color code reflects strength of neural similarity; size of circle indicates SEM. Left plot refers to high confidence trials; right plot shows data for low confidence trials.

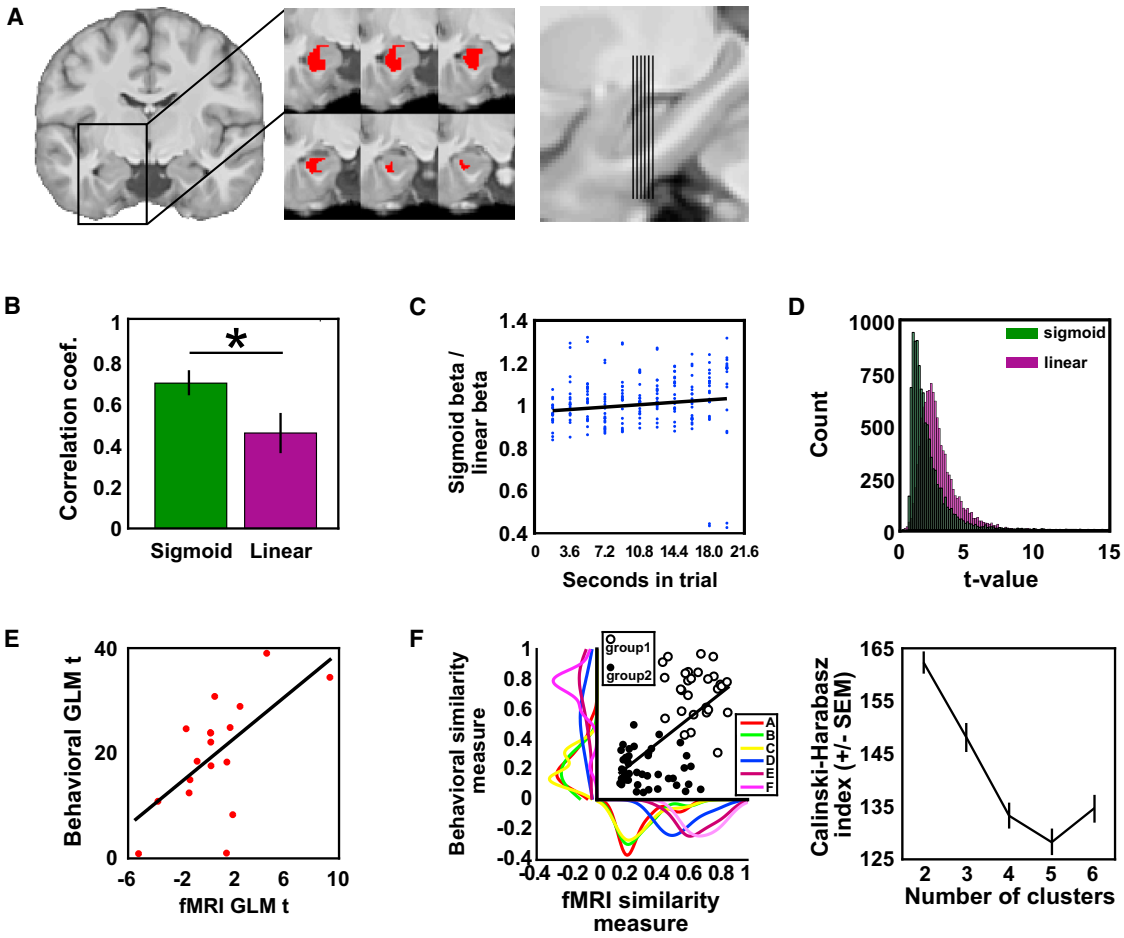

Figure 4. Participants with the Strongest Sigmoidal Effect in Behavior Also Show the Strongest Sigmoidal Response Pattern in the Hippocampus

(A) Both behavioral similarity to base environments (ΔA/(ΔA+ΔF)) and multi-voxel fMRI pattern similarity measures were separately tested against a predictor matrix reflecting a canonical sigmoidal model using GLM, and the resulting t maps were correlated across participants (see Figure S4B). The same analysis was also performed using a canonical linear predictor matrix. Group effects for the sigmoidal model, restricted to hippocampal region of interest and thresholded at a bootstrap-corrected $p < 0.05$, are overlaid on a study-specific template. Shown is the extent of the hippocampal effect from $y = -16$ to $y = -10$ with slice locations shown on a sagittal plane. These results were not influenced by differences in navigational behavior or mean hippocampal BOLD signal across environments (see Figure S2).

(B) Bar plots show the correlation coefficients for the canonical sigmoidal and linear model at their peak voxel in the hippocampus ± SEM ($x = -39$, $y = -13$, $z = -21$; bootstrap-corrected $p < 0.05$).

(C) Multivoxel fMRI data surrounding the hippocampal peak voxel from (A) explained by the sigmoidal model relative to the linear model as trials progress (see Supplemental Experimental Procedures). A shift toward a dominantly sigmoidal fit over time was observed, reflected in a significant positive slope of the fit ratio during trial progression (linear regression: slope = 0.004, $p < 0.05$). The model predicts a fit ratio below 1 up to 5.4 s in the trial and above 1 after 9 s in the trial.

(D) Monte-Carlo simulation showing the adherence of the linear and sigmoidal model on randomly shuffled data; higher t values indicate a better fit. The distribution of t values from the linear model fits is wider and shifted to higher values compared to the t values from the sigmoidal model fits (Kolmogorov-Smirnov test: $p < 0.001$).

(E) Scatterplot shows individual t-values from the fMRI against the behavioral GLM using the sigmoidal prediction model for every participant in the hippocampal peak voxel.

(F) Similarity measures in each environment from both the fMRI and behavioral data are plotted against each other (see Supplemental Experimental Procedures). A significant positive correlation was observed between the two similarity measures (Pearson's correlation: $t_{18} = 3.372$, $p < 0.001$, $R = 0.622$). Environment-wise distribution curves are plotted separately on the x and y axis for the fMRI and behavioral similarity measure, respectively. K means cluster analysis revealed that a two-cluster separation resulted in the highest Calinski-Harabasz index value (right plot; error bars indicate SEM). The two clusters in the left plot are indicated by open and closed dots (group 1 and group 2) and are clearly separated along the diagonal. This suggests two basic patterns of data rather than a continuum, indicative of a concurrent sigmoidal pattern in behavioral and neural responses.

The putative neural process underlying the formation of hippocampal memories is remapping [19], the formation of distinct representations by populations of place cells in response to environmental change. Place-cell-based representations exhibit attractor-like dynamics (sharp transitions) when animals are exposed to similar novel environments that have features

mapping in between already known, distinct environments (differing in shape, color, and texture; [22]), but not if trained in environments that are less distinct [36]. Although it is infeasible to register place cell activity in humans using fMRI, given that the distribution of place cells in rodent hippocampus is non-topographic with respect to the spatial distribution of their firing fields [37], the aforementioned rodent place cell pattern shows striking similarities with our data. Our data are consistent with the absence of sigmoidal neural response patterns in the human hippocampus when participants view highly similar visual scenes [38, 39] and a linear scaling of hippocampal responses with changes in the configuration of landmarks in four virtual environments [40]. The attractor-like behavior of place cells also accords with observations in rodents that repeated exposure to less-distinct environments is accompanied by a slower, gradual development of distinct place cell representations [41]. However, the distribution of the place cell activity in different environments has not been examined in detail, and it is the similarity of activity in different environments that we examine with multi-voxel pattern analysis (MVPA) in our study. Our results might also relate to a recent observation by Agarwal et al. [42], showing that spatial information can be obtained from local field potentials (LFPs) in the rodent hippocampus, summating electrical activity of a large number of neurons, which more closely relates to the BOLD response obtained with fMRI. However, future translational studies are necessary to more directly understand the relationship between population activity of spatially tuned cells and the fMRI signal in the hippocampal formation.

How do nonlinear dynamics in the hippocampus relate to pattern separation, as for instance indexed by fMRI adaptation [43]? Pattern separation, albeit related, is not necessarily due to attractor dynamics. Pattern separation in the hippocampus might accentuate small differences, rather than being attracted to a different fixed point, like the familiar pattern of the baseline environments in the present study and in the work by Wills et al. [22]. In addition, although pattern separation has been observed during virtual reality navigation [44], putative attractor dynamics are characterized by the emergence of a nonlinear response profile over time (Figure 4C).

Could the presence of a sigmoidal effect in the fMRI pattern in the hippocampus be explained by something other than putative attractor dynamics? A nonlinear response profile as observed in the present study effectively reflects a thresholded tuning function. Here, we provide evidence for a sigmoidal pattern in both behavioral and multi-voxel fMRI data as well as in a brain-behavior interaction and also show the systematic emergence of the nonlinear response profile within trials. Taken together, these effects are indicative of putative attractor dynamics but ultimately not a necessary condition, and alternative processes could potentially explain the sigmoidal output function. Any such alternative must either include the differences in background images or the locations where objects are placed by participants, since these are the only features that change between environments. Eliminating same-object comparisons in our analysis does not influence our results; therefore, the drop locations and associated similarities of paths and background cues cannot drive the observed sigmoidal pattern (Figure S3A). Furthermore, in visual cortex we do see a linear response pattern rather than a sigmoidal pattern, making it further unlikely that mere visual differences between environments contribute to the observed effect (Figure 3C). In addition, naive participants perceive the background images to change linearly (Figure 2), and this perception could be used to make a binary choice on where to drop the cued object (i.e., if perceived more similar to A, recall environment A). This strategy would eliminate the need for putative attractor dynamics in the hippocampus and still show binary memory activation in fMRI data. However, it would not predict a change from a more linear to a more sigmoidal pattern within trials as seen in our data (see Figure 4C) or be congruent with earlier rodent studies [22].

In sum, the sigmoidal response pattern we observe in the hippocampus provides novel evidence for an abrupt, remapping-like response to a linearly changed spatial context in humans, consistent with a recent report showing consequences of such a response in multi-modal pattern completion [45] and with pattern separation and completion during memory disambiguation in virtual reality [44]. Participants were trained to ceiling so as to form distinct and separate memories for the two original environments. In addition, analyses of fMRI data acquired during the learning phase for a subset of our participants indicates that, like place cell remapping in less-distinct environments [41], representations of environments A and F in the hippocampus de-correlate as a function of learning such that distinct representations already emerge on day 1 and continue to diverge on day 2 (Figure S1; see Supplemental Experimental Procedures). This suggests that a certain level of distinctiveness between two representations is required to observe nonlinear dynamics between the morph environments.

In conclusion, our study provides evidence for putative attractor dynamics and spatial remapping in the human hippocampus and highlights that these neural mechanisms underpin memory-based decision making in novel situations.

SUPPLEMENTAL INFORMATION

Supplemental Information includes Supplemental Experimental Procedures and four figures and can be found with this article online at http://dx.doi.org/10.1016/j.cub.2016.04.063.

AUTHOR CONTRIBUTIONS

C.F.D., N.B., and C.B. conceived this research. C.F.D., C.B., B.S., and A.V.-G. designed the experiment. B.S., T.N.S., and A.V.-G. developed the experimental task and performed the fMRI experiment. P.S. performed the behavioral experiment. B.S., A.V.-G., and C.F.D. analyzed the data. C.F.D., B.S., T.N.S., N.B., C.B., and A.V.-G. wrote the paper. All authors discussed the results and contributed to the paper.

ACKNOWLEDGMENTS

This work was supported by European Research Council (ERC-StG 261177) and Netherlands Organization for Scientific Research (NWO-Vidi 452-12-009) fellowships awarded to C.F.D. N.B. is supported by the Wellcome Trust and the Medical Research Council, UK. C.B. is funded by the Wellcome Trust and the Royal Society, UK (101208/z/13/z). The authors would like to thank S. Auger and O. Vikbladh for earlier behavioral pilot work; S. Bosch for help with data acquisition; and A. Backus and J. Bellmund for useful discussions.

Received: August 29, 2015
Revised: April 18, 2016
Accepted: April 29, 2016
Published: June 23, 2016

REFERENCES

1. Hopfield, J.J. (1982). Neural networks and physical systems with emergent collective computational abilities. Proc. Natl. Acad. Sci. USA *79*, 2554–2558.
2. Marr, D. (1971). Simple memory: a theory for archicortex. Philos. Trans. R. Soc. Lond. B Biol. Sci. *262*, 23–81.
3. McClelland, J.L., McNaughton, B.L., and O'Reilly, R.C. (1995). Why there are complementary learning systems in the hippocampus and neocortex: insights from the successes and failures of connectionist models of learning and memory. Psychol. Rev. *102*, 419–457.
4. McNaughton, B.L., and Morris, R.G.M. (1987). Hippocampal synaptic enhancement and information storage within a distributed memory system. Trends Cogn. Sci. *10*, 408–415.
5. Norman, K.A., and O'Reilly, R.C. (2003). Modeling hippocampal and neocortical contributions to recognition memory: a complementary-learning-systems approach. Psychol. Rev. *110*, 611–646.
6. Doeller, C.F., King, J.A., and Burgess, N. (2008). Parallel striatal and hippocampal systems for landmarks and boundaries in spatial memory. Proc. Natl. Acad. Sci. USA *105*, 5915–5920.
7. Ekstrom, A.D., Kahana, M.J., Caplan, J.B., Fields, T.A., Isham, E.A., Newman, E.L., and Fried, I. (2003). Cellular networks underlying human spatial navigation. Nature *425*, 184–188.
8. Howard, L.R., Javadi, A.H., Yu, Y., Mill, R.D., Morrison, L.C., Knight, R., Loftus, M.M., Staskute, L., and Spiers, H.J. (2014). The hippocampus and entorhinal cortex encode the path and Euclidean distances to goals during navigation. Curr. Biol. *24*, 1331–1340.
9. Miller, J.F., Neufang, M., Solway, A., Brandt, A., Trippel, M., Mader, I., Hefft, S., Merkow, M., Polyn, S.M., Jacobs, J., et al. (2013). Neural activity in human hippocampal formation reveals the spatial context of retrieved memories. Science *342*, 1111–1114.
10. Morgan, L.K., Macevoy, S.P., Aguirre, G.K., and Epstein, R.A. (2011). Distances between real-world locations are represented in the human hippocampus. J. Neurosci. *31*, 1238–1245.
11. Spiers, H.J., and Maguire, E.A. (2006). Thoughts, behaviour, and brain dynamics during navigation in the real world. Neuroimage *31*, 1826–1840.
12. Wolbers, T., and Büchel, C. (2005). Dissociable retrosplenial and hippocampal contributions to successful formation of survey representations. J. Neurosci. *25*, 3333–3340.
13. Buckner, R.L. (2010). The role of the hippocampus in prediction and imagination. Annu. Rev. Psychol. *61*, 27–48, C1–C8.
14. Carr, V.A., Rissman, J., and Wagner, A.D. (2010). Imaging the human medial temporal lobe with high-resolution fMRI. Neuron *65*, 298–308.
15. Davachi, L. (2006). Item, context and relational episodic encoding in humans. Curr. Opin. Neurobiol. *16*, 693–700.
16. Eichenbaum, H., Yonelinas, A.P., and Ranganath, C. (2007). The medial temporal lobe and recognition memory. Annu. Rev. Neurosci. *30*, 123–152.
17. Hasselmo, M.E. (2012). How We Remember: Brain Mechanisms of Episodic Memory (Cambridge: MIT Press).
18. Shohamy, D., and Turk-Browne, N.B. (2013). Mechanisms for widespread hippocampal involvement in cognition. J. Exp. Psychol. Gen. *142*, 1159–1170.
19. Bostock, E., Muller, R.U., and Kubie, J.L. (1991). Experience-dependent modifications of hippocampal place cell firing. Hippocampus *1*, 193–205.
20. Jezek, K., Henriksen, E.J., Treves, A., Moser, E.I., and Moser, M.-B. (2011). Theta-paced flickering between place-cell maps in the hippocampus. Nature *478*, 246–249.
21. Knierim, J.J., and Zhang, K. (2012). Attractor dynamics of spatially correlated neural activity in the limbic system. Annu. Rev. Neurosci. *35*, 267–285.
22. Wills, T.J., Lever, C., Cacucci, F., Burgess, N., and O'Keefe, J. (2005). Attractor dynamics in the hippocampal representation of the local environment. Science *308*, 873–876.
23. Blumenfeld, B., Preminger, S., Sagi, D., and Tsodyks, M. (2006). Dynamics of memory representations in networks with novelty-facilitated synaptic plasticity. Neuron *52*, 383–394.
24. Quian Quiroga, R., Kraskov, A., Mormann, F., Fried, I., and Koch, C. (2014). Single-cell responses to face adaptation in the human medial temporal lobe. Neuron *84*, 363–369.
25. Rotshtein, P., Henson, R.N.A., Treves, A., Driver, J., and Dolan, R.J. (2005). Morphing Marilyn into Maggie dissociates physical and identity face representations in the brain. Nat. Neurosci. *8*, 107–113.
26. Doeller, C.F., Barry, C., and Burgess, N. (2010). Evidence for grid cells in a human memory network. Nature *463*, 657–661.
27. Marchette, S.A., Vass, L.K., Ryan, J., and Epstein, R.A. (2014). Anchoring the neural compass: coding of local spatial reference frames in human medial parietal lobe. Nat. Neurosci. *17*, 1598–1606.
28. Wolbers, T., Wiener, J.M., Mallot, H.A., and Büchel, C. (2007). Differential recruitment of the hippocampus, medial prefrontal cortex, and the human motion complex during path integration in humans. J. Neurosci. *27*, 9408–9416.
29. Norman, K.A., Polyn, S.M., Detre, G.J., and Haxby, J.V. (2006). Beyond mind-reading: multi-voxel pattern analysis of fMRI data. Trends Cogn. Sci. *10*, 424–430.
30. Eichenbaum, H., and Cohen, N.J. (2014). Can we reconcile the declarative memory and spatial navigation views on hippocampal function? Neuron *83*, 764–770.
31. Duncan, K., Sadanand, A., and Davachi, L. (2012). Memory's penumbra: episodic memory decisions induce lingering mnemonic biases. Science *337*, 485–487.
32. Guitart-Masip, M., Barnes, G.R., Horner, A., Bauer, M., Dolan, R.J., and Duzel, E. (2013). Synchronization of medial temporal lobe and prefrontal rhythms in human decision making. J. Neurosci. *33*, 442–451.
33. Kumaran, D., Summerfield, J.J., Hassabis, D., and Maguire, E.A. (2009). Tracking the emergence of conceptual knowledge during human decision making. Neuron *63*, 889–901.
34. Wimmer, G.E., and Shohamy, D. (2012). Preference by association: how memory mechanisms in the hippocampus bias decisions. Science *338*, 270–273.
35. Zeithamova, D., Dominick, A.L., and Preston, A.R. (2012). Hippocampal and ventral medial prefrontal activation during retrieval-mediated learning supports novel inference. Neuron *75*, 168–179.
36. Leutgeb, J.K., Leutgeb, S., Treves, A., Meyer, R., Barnes, C.A., McNaughton, B.L., Moser, M.-B., and Moser, E.I. (2005). Progressive transformation of hippocampal neuronal representations in "morphed" environments. Neuron *48*, 345–358.
37. Redish, A.D. (2001). The hippocampal debate: are we asking the right questions? Behav. Brain Res. *127*, 81–98.
38. Bonnici, H.M., Chadwick, M.J., Kumaran, D., Hassabis, D., Weiskopf, N., and Maguire, E.A. (2012a). Multi-voxel pattern analysis in human hippocampal subfields. Front. Hum. Neurosci. *6*, 290.
39. Bonnici, H.M., Kumaran, D., Chadwick, M.J., Weiskopf, N., Hassabis, D., and Maguire, E.A. (2012b). Decoding representations of scenes in the medial temporal lobes. Hippocampus *22*, 1143–1153.
40. Stokes, J., Kyle, C., and Ekstrom, A.D. (2015). Complementary roles of human hippocampal subfields in differentiation and integration of spatial context. J. Cogn. Neurosci. *27*, 546–559.
41. Lever, C., Wills, T., Cacucci, F., Burgess, N., and O'Keefe, J. (2002). Long-term plasticity in hippocampal place-cell representation of environmental geometry. Nature *416*, 90–94.

42. Agarwal, G., Stevenson, I.H., Berényi, A., Mizuseki, K., Buzsáki, G., and Sommer, F.T. (2014). Spatially distributed local fields in the hippocampus encode rat position. Science *344*, 626–630.

43. Bakker, A., Kirwan, C.B., Miller, M., and Stark, C.E.L. (2008). Pattern separation in the human hippocampal CA3 and dentate gyrus. Science *319*, 1640–1642.

44. Kyle, C.T., Stokes, J.D., Lieberman, J.S., Hassan, A.S., and Ekstrom, A.D. (2015). Successful retrieval of competing spatial environments in humans involves hippocampal pattern separation mechanisms. eLife *4*, 4.

45. Horner, A.J., Bisby, J.A., Bush, D., Lin, W.-J., and Burgess, N. (2015). Evidence for holistic episodic recollection via hippocampal pattern completion. Nat. Commun. *6*, 7462.